IEEE Access
Multidisciplinary | Rapid Review | Open Access Journal

Received May 23, 2018, accepted June 17, 2018, date of publication June 25, 2018, date of current version July 19, 2018.

Digital Object Identifier 10.1109/ACCESS.2018.2849994

Robust Indirect Adaptive Control for a Class of Nonlinear Systems and Its Application to Shape Memory Alloy Actuators

BI ZHANG[1], XIN-GANG ZHAO[1], (Member, IEEE), XIAO-GUANG LI[1,2], AND DAO-HUI ZHANG[1]

[1]State Key Laboratory of Robotics, Shenyang Institute of Automation, Chinese Academy of Sciences, Shenyang 110016, China
[2]School of Chemical Equipment, Shenyang University of Technology, Shenyang 110870, China

Corresponding author: Xin-Gang Zhao (zhaoxingang@sia.cn)

This work was supported in part by the National High Technology Research and Development Program of China (863 Program) under Grant 2015AA042302 and in part by the National Natural Science Foundation of China under Grants 61773369 and 61573340.

ABSTRACT In this paper, a new robust adaptive control method has been proposed for nonlinear systems with uncertainties. This method combines the advantages of self-tuning control and sliding mode control. A simple parameterization model is first derived based on a linear dynamic model and unmodeled dynamics. Based on a modified sliding surface, the design procedure is based on the indirect adaptive control concept. This controller consists of four parts: 1) the system parameters estimation; 2) the unmodeled dynamics estimation; 3) the weighting polynomials updating; and 4) the control law calculation. The key merits of this controller are as follows: 1) the controller is applicable to non-minimum phase and open-loop unstable systems; 2) the estimation of the unmodeled dynamics is introduced as a feedback compensation control to improve the response; and 3) the strict stability condition is eliminated and a desirable performance is ensured during a wide operation region. Moreover, the control problem of a shape memory alloy actuator system is considered. In the literature, the mechanism model-based controllers have been extensively reported to address this issue. As an alternative, we describe this plant as a gray-box model. The adaptation algorithm and the control law have been implemented through the Beckhoff controller. The experimental results have demonstrated that the proposed controller has wider applicability than some existing methods.

INDEX TERMS Adaptive control, unmodeled dynamics, stability, robustness, SMA actuator.

I. INTRODUCTION

Adaptive control theory has been an active research topic since the last century. The key merit of an adaptive controller is that it is effective to the control problem of systems with uncertainties [1]. Self-tuning control [2] is one of the most common adaptive control strategies. Major advances have been made in the linear self-tuning control theory [3]–[7]. To meet the requirements of industrial plants, nonlinear self-tuning control schemes are studied to address the inherent nonlinear behaviors. Plenty of nonlinear models have been suggested for self-tuning controller design, such as neural networks [8], [9], fuzzy models [10], [11], multiple models [12], [13] and nonlinear autoregressive moving average with exogenous models [14], [15]. Despite the progresses achieved in the theoretical aspects, these interesting results suffer from the following critical drawbacks: (i) due to the complexities of nonlinear models and the uncertainties of their adaptations, the closed-loop stability analysis of nonlinear self-tuning control systems has always been very difficult and even intractable; (ii) the effectiveness of the output tracking is guaranteed by the assumption that the plants can be precisely described by the nonlinear models, which is difficult to satisfy in practice; (iii) the nonlinear self-tuning controller designs are quite implicit and cumbersome, in which the model structures are complicated, the identified parameters are increased, and the computational burdens are undesirable. Consequently, the theoretical results may have less potential for applications.

In our view, there is still a long way from finding increased applications for self-tuning adaptive control strategies. Such a situation is mainly due to the lack of systematic methodology that can enhance the robustness property of the

overall system. Essentially, the robustness property has always been a major concern, as important as the closed-loop stability and the output tracking performance. It has been a consensus that when there exist model mismatch, unmodeled dynamics and non-Gaussian disturbances [16], a conventional adaptive controller may cause undesirable performance. Some reports have considered robust self-tuning control problems by treating the modeling errors as bounded disturbances [17], [18]. Though the robustness property has increased, it also results in performance degradation since the estimator is insensitive to uncertainties. Chen and Narendra [19] have proposed a compensation control strategy by the use of neural networks and multiple models. However, the control design procedure seems to be costly. It would be meaningful if we can find out an appropriate way to enhance the robustness property without affecting the output tracking performance.

The main issue addressed in this paper is: how could system robustness be ensured in a self-tuning adaptive control system? Interestingly, the sliding mode control theory exhibits excellent robustness to system uncertainties [20]. Thus to take advantage of the robustness of sliding mode control, meanwhile cope with the uncertainties of industrial plants, a favored approach is to combine the self-tuning control with the sliding mode control [21]–[26]. Furuta [21] presented a sliding mode adaptive control framework for the systems with unknown parameters, where the control signal is composed of a linear feedback term and a switching term with the equivalent control region. Chen *et al.* [23] proposed a non-switching adaptive sliding mode control for uncertain systems. This elegant control scheme is extended to a multivariable case [24] and cascade systems with hysteresis nonlinearities [25], [26]. Nevertheless, there remain some issues to be addressed in this field: (i) a fundamental assumption of these results is that the system is minimum phase, which greatly confines the applicability of the results; (ii) the sliding surface has fixed weighting terms which often has to satisfy some strict stability conditions and requires a trivial cut and try procedure; (iii) the methods are based on the direct adaptive control, which defines an extended model for controller design, which leads to a growth in the number of parameters to be estimated; (iv) the robust sliding mode control design may reduce the adaptive performance, and deteriorate the output tracking property.

This paper develops a more practical self-tuning adaptive sliding mode control strategy for nonlinear systems. Based on a simple parameterization model, the control strategy consists of four parts: the system parameters estimation, the unmodeled dynamics estimation, the weighting polynomials updating and the control law calculation. The closed-loop system stability is achieved under mild conditions. For the theoretical aspects, the main contributions of this paper are summarized as follows: (i) Based on a novel sliding surface, the controller is applicable to non-minimum phase and open-loop unstable systems; (ii) The weighting polynomials of the sliding surface are updated online such that the strict closed-loop stability condition is eliminated and a desirable control performance is guaranteed during the whole operation region; (iii) The controller design is based on the indirect adaptive control strategy [27], which identifies the controlled plant directly and thus ensures good convergence of the weighing polynomials updating; (iv) The estimation of the unmodeled dynamics is introduced as a feedback compensation control to improve the output tracking performance; (v) Taking all these factors (*i.e.* the indirect adaptive control design, the updating of weighing polynomials and the additional feedback compensation control) into considerations, the manner in which the closed-loop stability analysis is carried out forms a major contribution.

What is more, the proposed adaptive controller is applied to a shape memory alloy (SMA) actuator in the experimental study. SMA is a smart metallic material that happens transformation from thermal energy to mechanical energy when it is heated up to an appropriate temperature [28]. SMA actuators have some advantages such as high power to mass ratio, maintainability, reliability, biocompatibility, light weight, and silent actuation [29]. These remarkable electrical and mechanical properties in solving engineering problems enable SMAs to serve as an alternative to replace conventional actuators. SMA achieves actuation via the transformation between the Martensite phase (cold) and the Austenite phase (hot). The SMA shape can be easily deformed by external stress in the Martensite phase, and the original shape can be recovered by heating SMA to the Austenite phase. It is reported that the SMAs have been used in plenty of practical applications such as biomedical engineering [30], aerospace applications [31], automotive applications [32], and robotic applications [33]. Despite of the salient features, it is a consensus that for SMA actuators there exist nonlinearities, parameter uncertainties, hysteresis, slow response speed and difficulty in measuring intermediate variables (*i.e.* temperature). The above disadvantages have made SMA actuators difficult to model and control.

In the literature, most of the successful controllers for SMA actuators are based on the sliding mode control approach. Romano and Tannuri [34] have designed a SMA actuator with a cooling system, established a mathematical model and derived a robust sliding mode controller. Ashrafiuon and Jala [35] have designed a novel sliding mode controller incorporating with an extended Kalman filter, which estimates the states of the plant. Pai *et al.* [36] have introduced a novel strategy for precision control of SMA actuator by combining a temperature controller and a sliding mode controller. Tai and Ahn [37] have built up a radial basis function neural network (RBFNN) based model for the SMA actuator, and then based on the black-box model a NN controller is developed. For an antagonistic SMA actuator, Wiest and Bucker [38] have employed recurrent NNs for the hysteresis compensation and proposed an indirect intelligent sliding mode control scheme. Nikdel *et al.* [39] have designed a new SMA based manipulator, and compared the sliding mode controller with the NN model predictive controller.

Meanwhile, adaptive control also provides a new look to dealing with the nonlinearities of SMA actuators, such as [40]–[42]. In sum, most of these schemes focus on mechanism models [34]–[36], [40], [41], which are inaccurate due to severe uncertainties. Some other publications also introduce neural networks models [37]–[39], [42], but the computational complexities are often high and the local minimum value problems remain an issue.

In this research, an alternative modeling and control scheme will be implemented to the SMA actuated system. Based on the input current and the output displacement, the SMA actuator is described as a gray-box model. It is noted that no intermediate variables (*i.e.* temperature) are required to be measured. Then the model parameters together with the unmodeled dynamics are updated by the recursive estimator, which requires a quite low computational burden and thus is usable for online control. The weighing polynomials updating will be employed for the purpose of fast response when the operation condition changes, while the weighing polynomials will keep unchanged for the robustness considerations under load variations and stochastic disturbances. The recursive algorithms and the control law have been implemented through the Beckhoff controller (which is a real time industrial PC-based controller and possesses several advantages such as high reliability, satisfactory extensibility, excellent compatibility and open platform). The experimental results indicate that the proposed controller is effective, and has a promising potential in many practical applications, which is another contribution of this work.

II. PROBLEM FORMULATION

Consider the discrete-time, nonlinear dynamical system described in the single-input-single-output (SISO) form

$$y(t+1) = f\left[y(t), \ldots, y(t+1-n_a), u(t), \ldots, u(t+1-n_b)\right] \tag{1}$$

where $u(t)$ and $y(t)$ are the system input and output signals; n_a and n_b are the system orders; $f[\cdot]$ is the smooth nonlinear function. The origin is considered as an equilibrium point.

The nonlinear system (1) can be equivalently represented as the following equation by linearization using Taylor's formula around the origin. Similar to [23], we consider the system (2) described by

$$A(z^{-1})y(t+1) = B(z^{-1})u(t) + \zeta\left[y(t), \ldots, y(t+1-n_a), u(t), \ldots, u(t+1-n_b)\right] \tag{2}$$

where $A(z^{-1})$ and $B(z^{-1})$ are polynomials in the unit time delay operator z^{-1} $\left\{e.g.\ z^{-1}u(t) = u(t-1)\right\}$ which are defined as follows

$$A(z^{-1}) = 1 + a_1 z^{-1} + a_2 z^{-2} + \ldots + a_{n_a} z^{-n_a}$$
$$B(z^{-1}) = b_1 + b_2 z^{-1} + \ldots + b_{n_b} z^{-n_b+1}$$

where $a_1, a_2, \ldots, a_{n_a}, b_1, b_2, \ldots, b_{n_b}$ are unknown parameters; $\zeta[\cdot]$ is the higher order smooth nonlinear function with respect to $y(t), \ldots, y(t+1-n_a), u(t), \ldots, u(t+1-n_b)$. For simplicity, the term $\zeta[y(t), \ldots, y(t+1-n_a), u(t), \ldots, u(t+1-n_b)]$ is written as $\zeta(t)$, which will be called "unmodeled dynamics" in this work.

The objectives are to produce a control input such that the system output tracks the reference, and to guarantee the robust stability of the closed-loop system despite of uncertainties.

The following assumptions are imposed on the system (2).

Assumption 1: The orders n_a and n_b are known.

Assumption 2: The nonlinearity $\zeta(t)$ satisfies

$$|\zeta(t)| \le \sigma \tag{3}$$

where σ is an **unknown** positive coefficient.

Remark 1: Note that the plant is not restricted to be minimum phase. The robust stability of the proposed controller will be proved based on the generalized minimum variance control [2].

III. ADAPTIVE CONTROL ALGORITHMS

As depicted in Fig. 1, an indirect adaptive control scheme is introduced. This strategy separates the control law calculation from the online adaptation algorithm.

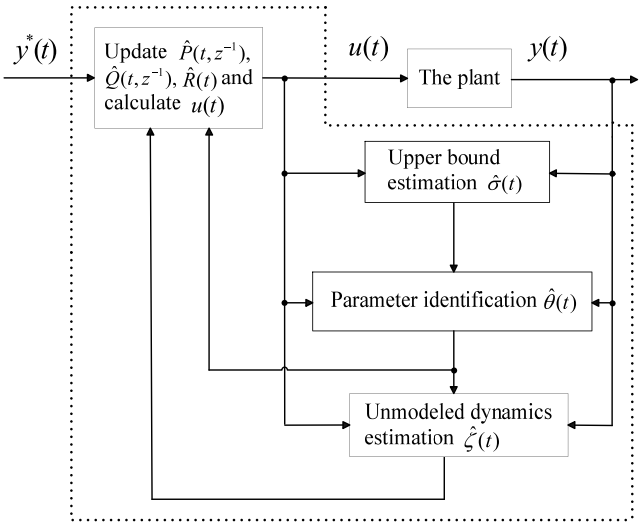

FIGURE 1. The robust indirect adaptive sliding mode control scheme.

A. SLIDING SURFACE FOR COMPLETELY KNOWN SYSTEMS

The following sliding surface is usually employed for the controller design [43]

$$s(t+1) = P(z^{-1})y(t+1) + Q(z^{-1})u(t) - Ry^*(t+1) \tag{4}$$

where $y^*(t)$ is a bounded reference; the user-chosen weighting polynomials $P(z^{-1}) = p_0 + p_1 z^{-1} + \ldots + p_{n_p} z^{-n_p}$ and $Q(z^{-1}) = q_0 + q_1 z^{-1} + \ldots + q_{n_q} z^{-n_q}$ are with orders n_p and n_q; R is a weighting coefficient. The terms $P(z^{-1})$, $Q(z^{-1})$ and R are pre-specified and fixed in the conventional adaptive sliding mode controller [43]. In general, $P(z^{-1})$ is chosen to be a stable polynomial.

For completely known plants, to achieve the desired control objective $s(t+1)=0$, the control law is as follow

$$T(z^{-1})u(t) = Ry^*(t+1) - S(z^{-1})y(t) - p_0\zeta(t) \quad (5)$$

where $S(z^{-1}) = s_1 + s_2z^{-1} + \ldots + s_{n_s}z^{-n_s+1}$ and $T(z^{-1}) = t_1 + t_2z^{-1} + \ldots + t_{n_t}z^{-n_t+1}$. Both of the parameters $(s_1, s_2, \ldots, s_{n_s}, t_1, t_2, \ldots, t_{n_t})$ and the orders (n_s, n_t) are determined by $P(z^{-1}) = p_0A(z^{-1}) + z^{-1}S(z^{-1})$ and $T(z^{-1}) = p_0B(z^{-1}) + Q(z^{-1})$.

By substituting the desired relationship $s(t+1)=0$ into the system (5), we can obtain the closed-loop equation

$$\left[P(z^{-1})B(z^{-1}) + Q(z^{-1})A(z^{-1})\right]y(t+1) = B(z^{-1})Ry^*(t+1) + Q(z^{-1})\zeta(t) \quad (6)$$

The equation (6) indicates that, for a completely known system, to achieve the closed-loop stability, the weighting polynomials $P(z^{-1})$ and $Q(z^{-1})$ should be properly chosen to guarantee that $\left[P(z^{-1})B(z^{-1}) + Q(z^{-1})A(z^{-1})\right]$ is stable [43]. However, when system parameters are uncertain, it is difficult to offline choose appropriate $P(z^{-1})$ and $Q(z^{-1})$ to ensure this restrict condition for distinct operation regions. To remove the above assumption, a more favored treatment is to update $P(z^{-1})$ and $Q(z^{-1})$ online based on some prescribed poles [27]. In the *Control Law Design* subsection, we will show that the choices of these weighing terms can be online updated.

B. RECURSIVE ESTIMATOR

Online adaptation algorithm will be introduced to identify the uncertain system (2).

To construct an identification model, the system (2) can be rewritten compactly as follow

$$y(t) = \varphi^T(t)\theta + \zeta(t) \quad (7)$$

where the parameter vector θ and the regressor vector $\varphi(t)$ are defined as follows

$$\theta = \left[b_1, b_2, \ldots, b_{n_b}, a_1, a_2, \ldots, a_{n_a}\right]^T \quad (8)$$

$$\varphi(t) = [u(t-1), u(t-2), \ldots, u(t-n_b), -y(t-1), -y(t-2), \ldots, -y(t-n_a)]^T \quad (9)$$

Then we have the following identification model

$$y(t+1) \triangleq \varphi^T(t+1)\hat{\theta}(t) \quad (10)$$

with $\hat{\theta}(t)$ defined as the estimation of θ

$$\hat{\theta}(t) = \left[\hat{b}_1(t), \hat{b}_2(t), \ldots, \hat{b}_{n_b}(t), \hat{a}_1(t), \hat{a}_2(t), \ldots, \hat{a}_{n_a}(t)\right]^T \quad (11)$$

Let $\hat{\sigma}(t)$ be the estimation of σ.

The uncertain parameters $\hat{\theta}(t)$ and $\hat{\sigma}(t)$ are updated by the following modified recursive stochastic gradient identification algorithm with a deadzone weighted factor

$$e(t) = y(t) - \varphi^T(t)\hat{\theta}(t-1) \quad (12)$$

$$r(t) = r(t-1) + \varphi^T(t)\varphi(t) \quad (13)$$

$$\lambda(t) = \begin{cases} 1 - \hat{\sigma}(t-1)/|e(t)|, & \text{if } |e(t)| > \hat{\sigma}(t-1) \\ 0, & \text{otherwise} \end{cases} \quad (14)$$

$$\hat{\theta}(t) = \hat{\theta}(t-1) + \frac{\varepsilon\lambda(t)\varphi(t)e(t)}{r(t)} \quad (15)$$

$$\hat{\sigma}(t) = \hat{\sigma}(t-1) + \frac{\varepsilon\lambda(t)|e(t)|}{r(t)} \quad (16)$$

where $r(0)=1$; $\hat{\sigma}(t)$ is the estimation of the upper bound σ; $e(t)$ is the model error; $\lambda(t)$ is a nonnegative weighted factor; ε is a user-designed adaptation gain and satisfies $0 < \varepsilon \leq 2$ (*Lemma 1* will explain the reason).

Remark 2: In this recursive estimator, the weighted factor $\lambda(t)$ can effectively increase the system robustness especially when the uncertainties cannot be neglected. But on the other hand, the weighted factor $\lambda(t)$ may also lead to undesirable ''insensitivity'' in the parameters updating. Thus a compromise has to be made between the system robustness and the control performance.

In order to achieve better control performance, efforts should be made to compensate for the unmodeled dynamics $\zeta(t)$. Let $\hat{\zeta}(t)$ be denoted as the estimation of $\zeta(t)$, which is updated by

$$\hat{\zeta}(t) = y(t) - \varphi^T(t)\hat{\theta}(t) \quad (17)$$

Then the estimation $\hat{\zeta}(t)$ will be employed as a compensation in the controller design.

Remark 3: Note that the aims of the estimates $\hat{\sigma}(t)$ and $\hat{\zeta}(t)$ are different. The former one is for the robust identification of system parameters, while the latter is to add an compensation control when the estimator is insensitive to uncertainties.

C. CONTROL LAW DESIGN

Based on (11), the estimated polynomials at instant t can be defined as

$$\hat{A}(t, z^{-1}) = 1 + \hat{a}_1(t)z^{-1} + \hat{a}_2(t)z^{-2} + \ldots + \hat{a}_{n_a}(t)z^{-n_a}$$
$$\hat{B}(t, z^{-1}) = \hat{b}_1(t) + \hat{b}_2(t)z^{-1} + \ldots + \hat{b}_{n_b}(t)z^{-n_b+1}$$

Along with (4), $\hat{P}(t, z^{-1})$, $\hat{Q}(t, z^{-1})$ and $\hat{R}(t)$ are defined in replace of $P(z^{-1})$, $Q(z^{-1})$ and R. The polynomials $\hat{P}(t, z^{-1}) = \hat{p}_0(t) + \hat{p}_1(t)z^{-1} + \ldots + \hat{p}_{n_p}(t)z^{-n_p}$ and $\hat{Q}(t, z^{-1}) = \hat{q}_0(t) + \hat{q}_1(t)z^{-1} + \ldots + \hat{q}_{n_q}(t)z^{-n_q}$ are online updated based on the following equation [27]

$$\Gamma(z^{-1}) = \hat{P}(t, z^{-1})\hat{B}(t, z^{-1}) + \hat{Q}(t, z^{-1})\hat{A}(t, z^{-1}) \quad (18)$$

where $\Gamma(z^{-1})$ is a pre-specified **stable** polynomial. Now the modified sliding surface is expressed as follow

$$s(t+1) = \hat{P}(t, z^{-1})y(t+1) + \hat{Q}(t, z^{-1})u(t) - \hat{R}(t)y^*(t+1) \quad (19)$$

Then based on (5) and the adaptation algorithm (12)-(18), the control law is as follow

$$\hat{T}(t, z^{-1})u(t) = \hat{R}(t)y^*(t+1) - \hat{S}(t, z^{-1})y(t) - \hat{p}_0(t)\chi(t)\hat{\zeta}(t) \quad (20)$$

with $\hat{S}(t,z^{-1}) = \hat{s}_1(t) + \hat{s}_2(t)z^{-1} + \ldots + \hat{s}_{n_s}(t)z^{-n_s+1}$ and $\hat{T}(t,z^{-1}) = \hat{t}_1(t) + \hat{t}_2(t)z^{-1} + \ldots + \hat{t}_{n_t}(t)z^{-n_t+1}$ determined by $\hat{P}(t,z^{-1}) = \hat{p}_0(t)\hat{A}(t,z^{-1}) + z^{-1}\hat{S}(t,z^{-1})$ and $\hat{T}(t,z^{-1}) = \hat{p}_0(t)\hat{B}(t,z^{-1}) + \hat{Q}(t,z^{-1})$. In (20), the parameter $\chi(t)$ is defined as

$$\chi(t) = \begin{cases} 0, & \text{if } |e(t)| > \bar{\chi} \cdot \hat{\eta}(t-1) \\ 1, & \text{otherwise} \end{cases} \quad \text{where } \bar{\chi} > 1 \tag{21}$$

Remark 4: The modified sliding surface (19) is updated online for the purpose of a better performance. At each instant, the calculation of the elements $\left(\hat{p}_0(t), \hat{p}_1(t), \ldots, \hat{q}_0(t), \hat{q}_1(t), \ldots\right)$ is based on the pole assignment concept [27].

Remark 5: To eliminate steady-state output tracking errors, a straightforward way is to choose $\hat{R}(t) = \hat{P}(t,1)$ and $\hat{Q}(t,1) = 0$. Clearly, the former relationship is easy to be met by setting $\hat{R}(t) = \hat{p}_0(t) + \hat{p}_1(t) + \ldots + \hat{p}_{n_p}(t)$. For the latter one, $\hat{Q}(t,z^{-1})$ is suggested to be $\hat{Q}(t,z^{-1}) = \hat{Q}'(t,z^{-1})(1-z^{-1})$ for a polynomial $\hat{Q}'(t,z^{-1})$.

Remark 6: The parameter $\chi(t)$ is adopted to improve the system response. Clearly, when the estimation is not precise, no compensation is introduced for the unmodeled dynamics; when the estimation error is within a certain region, the compensation $\hat{\zeta}(t)$ is used for the feedback.

D. OVERALL ADAPTIVE CONTROL SCHEME

In short, the proposed robust indirect adaptive sliding mode control (RIASMC) scheme is summarized as follows:

Step 1: Collect $\{u(t), y(t)\}$ and construct $\varphi(t)$ by (9);
Step 2: Update $\hat{\theta}(t)$, $\hat{\sigma}(t)$, $\hat{\zeta}(t)$ by (12)-(17);
Step 3: Calculate $\hat{P}(t,z^{-1})$, $\hat{Q}(t,z^{-1})$, $\hat{R}(t)$ by (18);
Step 4: Calculate $u(t)$ by solving the equation (20);
Step 5: Let $t = t+1$ and apply $u(t)$ to the system (1).

IV. THEORETICAL ANALYSIS

The time-varying operation is indispensable for analyzing the closed-loop stability of an indirect adaptive control [27]. To simplify this concept, the following definition is introduced.

Definition 1: For the given time-varying polynomials

$$L(t,z^{-1}) = l_0(t) + l_1(t)z^{-1} + \ldots + l_{n_l}(t)z^{-n_l},$$
$$M(t,z^{-1}) = m_0(t) + m_1(t)z^{-1} + \ldots + m_{n_m}(t)z^{-n_m},$$

we define

$$L(t,z^{-1})M(t,z^{-1}) := \sum_{i=0}^{n_l}\sum_{j=0}^{n_m} l_i(t)m_j(t)z^{-i-j},$$
$$L(t,z^{-1}) \bullet M(t,z^{-1}) := \sum_{i=0}^{n_l}\sum_{j=0}^{n_m} l_i(t)m_j(t-i)z^{-i-j}.$$

Lemma 1: The adaptation algorithm (12)-(16) ensures the following properties:

$$\lim_{t\to\infty} \frac{\lambda^2(t)e^2(t)}{r(t)} = 0 \tag{22}$$

$$\lim_{t\to\infty} ||\hat{\theta}(t) - \hat{\theta}(t-1)|| = 0, \quad \lim_{t\to\infty} ||\hat{\sigma}(t) - \hat{\sigma}(t-1)|| = 0 \tag{23}$$

$$\hat{\theta}(t), \quad \hat{\sigma}(t) \text{ are bounded for any } t. \tag{24}$$

Proof: Define the function $V(t) = \tilde{\theta}^T(t)\tilde{\theta}(t) + \tilde{\sigma}^2(t)$, where $\tilde{\theta}(t) = \hat{\theta}(t) - \theta$, $\tilde{\sigma}(t) = \hat{\sigma}(t) - \sigma$.

Then consider the equation (25)

$$\begin{aligned} V(t) - V(t-1) &= \frac{2\varepsilon\lambda(t)\left\{e(t)\varphi^T(t)\tilde{\theta}(t-1) + |e(t)|\,\tilde{\sigma}(t-1)\right\}}{r(t)} \\ &\quad + \frac{\varepsilon^2\lambda^2(t)\left\{e(t)\varphi^T(t)\varphi(t)e(t) + e^2(t)\right\}}{r^2(t)} \end{aligned} \tag{25}$$

From (14), there exists $V(t) = V(t-1)$ when $|e(t)| \le \hat{\sigma}(t-1)$. Now let us consider the case when $|e(t)| > \hat{\sigma}(t-1)$.

From (7) and (12), it is seen that $\varphi^T(t)\tilde{\theta}(t-1) = \zeta(t) - e(t)$. Further based on (3), we have

$$\begin{aligned} V(t) - V(t-1) \le{}& \frac{2\varepsilon\lambda(t)\left\{-e^2(t) + |e(t)|\,\hat{\sigma}(t-1)\right\}}{r(t)} \\ &+ \frac{\varepsilon^2\lambda^2(t)e^2(t)\left\{\varphi^T(t)\varphi(t) + 1\right\}}{r^2(t)} \end{aligned} \tag{26}$$

From (13), we have $r(t) = 1 + \sum_{k=1}^{t}\varphi^T(k)\varphi(k) \ge 1 + \varphi^T(t)\varphi(t)$. Meanwhile from (14), it is known $|e(t)| - \hat{\sigma}(t-1) \le \lambda(t)\,|e(t)|$. Based on these facts, the equation (26) can be written as

$$\begin{aligned} V(t) - V(t-1) &\le -\frac{2\varepsilon\lambda^2(t)e^2(t)}{r(t)} + \frac{\varepsilon^2\lambda^2(t)e^2(t)}{r(t)} \\ &= -\frac{(2-\varepsilon)\varepsilon\lambda^2(t)e^2(t)}{r(t)} \end{aligned} \tag{27}$$

Thus in order to ensure $V(t) - V(t-1) \le 0$, the coefficient ε must satisfy $0 < \varepsilon \le 2$.

Then there exists that

$$\sum_{k=1}^{t}(V(k) - V(k-1)) \le -(2-\varepsilon)\varepsilon\sum_{k=1}^{t}\frac{\lambda^2(k)e^2(k)}{r(k)} \tag{28}$$

Now combining (28) with the fact $V(t) \ge 0$ and following the same line as that in [2], the conclusions (22)-(24) can be proven. □

Lemma 2: Let Assumptions 1-2 hold and apply the adaptive control algorithms (12)-(18) and (20) to the nonlinear system (1), then there exist positive constants K_1, K_2 such that

$$\max_{0\le\tau\le t} ||\varphi(\tau)|| \le K_1 + K_2 \max_{0\le\tau\le t}\{\lambda(\tau)\,|e(\tau)|\} \tag{29}$$

Proof: From (9), (11) and (12), it is derived that

$$\begin{aligned} &e(t+1) \\ &= y(t+1) - \left\{\left[1 - \hat{A}(t,z^{-1})\right]y(t+1) + \hat{B}(t,z^{-1})u(t)\right\} \\ &= \hat{A}(t,z^{-1})y(t+1) - \hat{B}(t,z^{-1})u(t) \end{aligned} \tag{30}$$

Further combining (30) with (20) yields that

$$\begin{aligned}\hat{p}_0(t)e(t+1) &= \hat{p}_0(t)\hat{A}(t,z^{-1})y(t+1) + \hat{Q}(t,z^{-1})u(t) \\ &\quad - \hat{T}(t,z^{-1})u(t) \\ &= \hat{P}(t,z^{-1})y(t+1) + \hat{Q}(t,z^{-1})u(t) \\ &\quad - \hat{R}(t)y^*(t+1) + \hat{p}_0(t)\chi(t)\hat{\zeta}(t) \\ &= s(t+1) + \hat{p}_0(t)\chi(t)\hat{\zeta}(t) \end{aligned} \tag{31}$$

Meanwhile, from (7) and (17), it is obtained that

$$\hat{\zeta}(t) = \zeta(t) + \varphi^T(t)\left[\theta - \hat{\theta}(t)\right] \tag{32}$$

Then from (31) and (32), we have

$$\begin{aligned}&\hat{p}_0(t)e(t+1) \\ &\quad = \hat{P}(t,z^{-1})y(t+1) + \hat{Q}(t,z^{-1})u(t) - \hat{R}(t)y^*(t+1) \\ &\qquad + \hat{\Pi}(t) + \hat{p}_0(t)\chi(t)\zeta(t) \end{aligned} \tag{33}$$

where $\hat{\Pi}(t) = \hat{p}_0(t)\chi(t)\varphi^T(t)\left[\theta - \hat{\theta}(t)\right]$.

Combining (33) with (30) yields the following equations

$$\begin{aligned}&\left[\hat{P}(t,z^{-1})\hat{B}(t,z^{-1}) + \hat{Q}(t,z^{-1})\hat{A}(t,z^{-1})\right]y(t+1) \\ &= \Gamma(z^{-1})y(t+1) \\ &= \left[\hat{B}(t,z^{-1})\hat{p}_0(t) + \hat{Q}(t,z^{-1})\right]e(t+1) \\ &\quad + \hat{B}(t,z^{-1})\hat{R}(t)y^*(t+1) \\ &\quad + \left\{\hat{B}(t,z^{-1})\hat{P}(t,z^{-1}) - \hat{B}(t,z^{-1}) \bullet \hat{P}(t,z^{-1})\right\}y(t+1) \\ &\quad + \left\{\hat{Q}(t,z^{-1})\hat{A}(t,z^{-1}) - \hat{Q}(t,z^{-1}) \bullet \hat{A}(t,z^{-1})\right\}y(t+1) \\ &\quad + \left\{\hat{Q}(t,z^{-1}) \bullet \hat{B}(t,z^{-1}) - \hat{B}(t,z^{-1}) \bullet \hat{Q}(t,z^{-1})\right\}u(t) \\ &\quad - \hat{B}(t,z^{-1})\hat{\Pi}(t) - \hat{B}(t,z^{-1})\hat{p}_0(t)\chi(t)\zeta(t) \end{aligned} \tag{34}$$

$$\begin{aligned}&\left[\hat{P}(t,z^{-1})\hat{B}(t,z^{-1}) + \hat{Q}(t,z^{-1})\hat{A}(t,z^{-1})\right]u(t) \\ &= \Gamma(z^{-1})u(t) \\ &= \left[\hat{A}(t,z^{-1})\hat{p}_0(t) - \hat{P}(t,z^{-1})\right]e(t+1) \\ &\quad + \hat{A}(t,z^{-1})\hat{R}(t)y^*(t+1) \\ &\quad + \left\{\hat{P}(t,z^{-1})\hat{B}(t,z^{-1}) - \hat{P}(t,z^{-1}) \bullet \hat{B}(t,z^{-1})\right\}u(t) \\ &\quad + \left\{\hat{A}(t,z^{-1})\hat{Q}(t,z^{-1}) - \hat{A}(t,z^{-1}) \bullet \hat{Q}(t,z^{-1})\right\}u(t) \\ &\quad + \left\{\hat{P}(t,z^{-1}) \bullet \hat{A}(t,z^{-1}) - \hat{A}(t,z^{-1}) \bullet \hat{P}(t,z^{-1})\right\}y(t+1) \\ &\quad - \hat{A}(t,z^{-1})\hat{\Pi}(t) - \hat{A}(t,z^{-1})\hat{p}_0(t)\chi(t)\zeta(t) \end{aligned} \tag{35}$$

From Lemma 1, it is clear that all the polynomials $\hat{A}(t,z^{-1})$, $\hat{B}(t,z^{-1})$, $\hat{P}(t,z^{-1})$, $\hat{Q}(t,z^{-1})$ and $\hat{R}(t)$ must have bounded coefficients. Meanwhile, when $t \to \infty$, the elements in the braces on the right-hand side of (34)-(35) tend to zero.

Then we left-multiple $\Gamma^{-1}(z^{-1})$ on both sides of (34)-(35) and use the fact that $\Gamma(z^{-1})$ is a stable polynomial for further results. It is a concensus that the reference signal $y^*(t)$ must be bounded, and the growth rates [2] of $|y(t+1)|$ and $|u(t)|$ are not faster than the regressor vector $||\varphi(t)||$. By Lemma 1, we can conclude that $\hat{\Pi}(t)$ has the same growth rate with $||\varphi(t)||$.

Let us first consider the case when $\chi(t) = 1$ in (20).

Based on (34), (35) and the above analysis, we know that there exist positive constants $K_3^{'}, K_4^{'}, K_5^{'}, K_6^{'}, K_3^{''}, K_4^{''}, K_5^{''}, K_6^{''}$ such that

$$\begin{aligned}|y(t)| &\le K_3^{'} + K_4^{'} \max_{0\le\tau\le t}|e(\tau)| \\ &\quad + K_5^{'} \max_{0\le\tau\le t}\|\varphi(\tau)\| + K_6^{'} \max_{0\le\tau\le t}|\zeta(\tau)| \end{aligned} \tag{36}$$

$$\begin{aligned}|u(t-1)| &\le K_3^{''} + K_4^{''} \max_{0\le\tau\le t}|e(\tau)| \\ &\quad + K_5^{''} \max_{0\le\tau\le t}\|\varphi(\tau)\| + K_6^{''} \max_{0\le\tau\le t}|\zeta(\tau)| \end{aligned} \tag{37}$$

Based on (9), it can be concluded that there exist positive constants K_3, K_4, K_5, K_6 such that

$$\begin{aligned}\max_{0\le\tau\le t}||\varphi(\tau)|| &\le K_3 + K_4 \max_{0\le\tau\le t}|e(\tau)| \\ &\quad + K_5 \max_{0\le\tau\le t}\|\varphi(\tau)\| + K_6 \max_{0\le\tau\le t}|\zeta(\tau)| \end{aligned} \tag{38}$$

Thus if we denote $\bar{K}_5 = 1$, then for any $0 < K_5 < \bar{K}_5$, it is concluded that there exist positive constants K_7, K_8, K_9 such that

$$\begin{aligned}&\max_{0\le\tau\le t}||\varphi(\tau)|| \\ &\le \frac{K_3}{1-K_5} + \frac{K_4}{1-K_5}\max_{0\le\tau\le t}|e(\tau)| + \frac{K_6}{1-K_5}\max_{0\le\tau\le t}|\zeta(\tau)| \\ &= K_7 + K_8 \max_{0\le\tau\le t}|e(\tau)| + K_9 \max_{0\le\tau\le t}|\zeta(\tau)| \end{aligned} \tag{39}$$

Then from Assumption 2, it is concluded that there exist positive constants K_8, K_{10} such that

$$\begin{aligned}\max_{0\le\tau\le t}||\varphi(\tau)|| &\le (K_7 + K_9\sigma) + K_8 \max_{0\le\tau\le t}|e(\tau)| \\ &= K_{10} + K_8 \max_{0\le\tau\le t}|e(\tau)| \end{aligned} \tag{40}$$

By using the property $|e(t)| - \hat{\sigma}(t-1) \le \lambda(t)|e(t)|$ defined in (14) again, it is obvious that

$$\begin{aligned}&\max_{0\le\tau\le t}||\varphi(\tau)|| \\ &\le K_{10} + K_8 \max_{0\le\tau\le t}\left\{|e(\tau)| - \hat{\sigma}(t-1) + \hat{\sigma}(t-1)\right\} \\ &\le K_{10} + K_8 \max_{0\le\tau\le t}\{\lambda(\tau)|e(\tau)|\} + K_8 \max_{0\le\tau\le t}\hat{\sigma}(t-1) \end{aligned} \tag{41}$$

From (24), it is known that there exist positive constants K_1, K_2 such that

$$\max_{0\le\tau\le t}||\varphi(\tau)|| \le K_1 + K_2 \max_{0\le\tau\le t}\{\lambda(\tau)|e(\tau)|\} \tag{42}$$

Obviously, Lemma 3 is also guaranteed under the case when $\chi(t) = 0$. The corresponding proof is similar to (36)-(42). □

Theorem 1: Assume that the nonlinear system (1) satisfies Assumptions 1-2. For the closed-loop system (7) with the adaptation algorithm (12)-(18) and the control law (20), the following conclusions are obtained.

(i) The closed-loop system is stable in the sense that all the signals are uniformly bounded. There also exists a small upper bound $\bar{\Delta}$ such that the output tracking error satisfies

$$\lim_{t\to\infty} \left|y(t) - y^*(t)\right| \le \bar{\Delta} \tag{43}$$

(ii) Moreover, if at the steady state, the unmodeled dynamics $\zeta(t)$ and the reference $y^*(t)$ are slowly varying with respect to the sampling frequency such that [24]

$$\zeta(t) \approx \zeta(t-1) \approx \ldots \approx \zeta(t-N) \tag{44}$$

$$y^*(t) \approx y^*(t-1) \approx \ldots \approx y^*(t-N) \tag{45}$$

can hold for a large integer N, then the output tracking error satisfies

$$\lim_{t\to\infty} \left|y(t) - y^*(t)\right| \approx 0 \tag{46}$$

Proof:

(i) Using (22), (29) and the "key technical Lemma" of [2, Lemma 6.2.1], two propositions can be obtained as follows: 1) $\{\lambda(t)\,|e(t)|\}$ is a bounded sequence and 2) $\lim_{t\to\infty} \lambda(t)\,|e(t)| = 0$.

From (42), the first proposition can be further extended to the following conclusions: $\{||\varphi(t)||\}$ is a bounded sequence, all the signals must be bounded and the closed-loop system is stable.

Based on the definition in (14), the second proposition means that $\lim_{t\to\infty} \sup\left\{|e(t)| - \hat{\sigma}(t-1)\right\} \le 0$. From (25), it is known that $\lim_{t\to\infty} \chi(t) = 1$. Combining (12) with (17) yields that

$$\hat{\zeta}(t) = e(t) + \varphi^T(t)\left[\hat{\theta}(t-1) - \hat{\theta}(t)\right] \tag{47}$$

Applying (47) to (31) yields that

$$\begin{aligned}
&\hat{p}_0(t)\,[e(t+1) - e(t)] \\
&\quad = \hat{P}(t, z^{-1})y(t+1) + \hat{Q}(t, z^{-1})u(t) - \hat{R}(t)y^*(t+1) \\
&\qquad + \hat{p}_0(t)\varphi^T(t)\left[\hat{\theta}(t-1) - \hat{\theta}(t)\right] \\
&\quad = s(t+1) + \hat{p}_0(t)\varphi^T(t)\left[\hat{\theta}(t-1) - \hat{\theta}(t)\right]
\end{aligned} \tag{48}$$

Then based on (23), (24), (48), $\hat{R}(t) = \hat{P}(t, 1)$, $\hat{Q}(t, 1) = 0$, and the fact that $\lim_{t\to\infty} \sup\left\{|e(t)| - \hat{\sigma}(t-1)\right\} \le 0$, we conclude that

$$\begin{aligned}
&\lim_{t\to\infty} \hat{p}_0(t)\,[e(t+1) - e(t)] \\
&= \lim_{t\to\infty} \left[\hat{P}(t, 1)y(t+1) - \hat{R}(t)y^*(t+1)\right] \\
&\quad + \lim_{t\to\infty} \hat{Q}(t, 1)u(t) + \lim_{t\to\infty} \hat{p}_0(t)\varphi^T(t)\left[\hat{\theta}(t-1) - \hat{\theta}(t)\right] \\
&= \lim_{t\to\infty} \left[\hat{P}(t, 1)y(t+1) - \hat{R}(t)y^*(t+1)\right] \\
&\Rightarrow \lim_{t\to\infty} \left|y(t) - y^*(t)\right| \le \bar{\Delta}
\end{aligned} \tag{49}$$

(ii) If the unmodeled dynamics $\zeta(t)$ and the reference $y^*(t)$ satisfy (44)-(45) at the steady state, then the system is governed by the external input $u(t)$, which indicates that the regressor vector $\varphi(t)$ is also slowly varying with respect to the samples [24]. Based on (7) and (12), it is concluded that $e(t)$ is also slowly varying with respect to the samples at the steady state, *i.e.*, $e(t) \approx e(t-1) \approx \ldots \approx e(t-N)$.

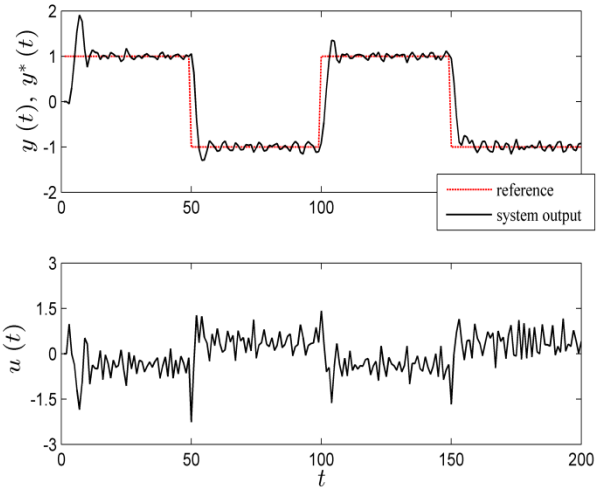

FIGURE 2. The output tracking $y(t)$ and control input $u(t)$.

Then based on (23), (24), (48), $\hat{R}(t) = \hat{P}(t, 1)$, $\hat{Q}(t, 1) = 0$ and the fact that $\lim_{t\to\infty} e(t) \approx \lim_{t\to\infty} e(t-1)$, we conclude that

$$\begin{aligned}
&\lim_{t\to\infty} \hat{p}_0(t)\,[e(t+1) - e(t)] \\
&= \lim_{t\to\infty} \left[\hat{P}(t, 1)y(t+1) - \hat{R}(t)y^*(t+1)\right] \\
&\quad + \lim_{t\to\infty} \hat{Q}(t, 1)u(t) + \lim_{t\to\infty} \hat{p}_0(t)\varphi^T(t)\left[\hat{\theta}(t-1) - \hat{\theta}(t)\right] \\
&= \lim_{t\to\infty} \left[\hat{P}(t, 1)y(t+1) - \hat{R}(t)y^*(t+1)\right] \approx 0 \\
&\Rightarrow \lim_{t\to\infty} \left|y(t) - y^*(t)\right| \approx 0
\end{aligned} \tag{50}$$

From (50), it is also found that the desired control objective $s(t+1) = 0$ is approximately achieved in the sense that

$$\begin{aligned}
&\lim_{t\to\infty} \hat{p}_0(t)\,[e(t+1) - e(t)] \\
&= \lim_{t\to\infty} s(t+1) + \lim_{t\to\infty} \hat{p}_0(t)\varphi^T(t)\left[\hat{\theta}(t-1) - \hat{\theta}(t)\right] \approx 0 \\
&\Rightarrow \lim_{t\to\infty} s(t+1) \approx 0
\end{aligned} \tag{51}$$

Meanwhile, from (16), (21) and (28), it is derived that

$$\lim_{t\to\infty} |\hat{\zeta}(t)| = \lim_{t\to\infty} |e(t)| \tag{52}$$

It is known that the model error $e(t)$ is actually induced by the unmodeled dynamics $\zeta(t)$. Equation (52) indicates that the control law (20) can gradually compensate this influence.

This proves Theorem 1. □

V. APPLICATION TO A SYNTHETIC NONLINEAR SYSTEM

Consider the following single-input-single-output discrete-time nonlinear dynamical system:

$$A(z^{-1})y(t+1) = B(z^{-1})u(t) + \zeta(t) \tag{53}$$

where $A(z^{-1}) = 1 - 2z^{-1} + 0.8z^{-2}$ and $B(z^{-1}) = 0.25 + 0.3z^{-1}$. The system (53) contains unstable poles and zeros.

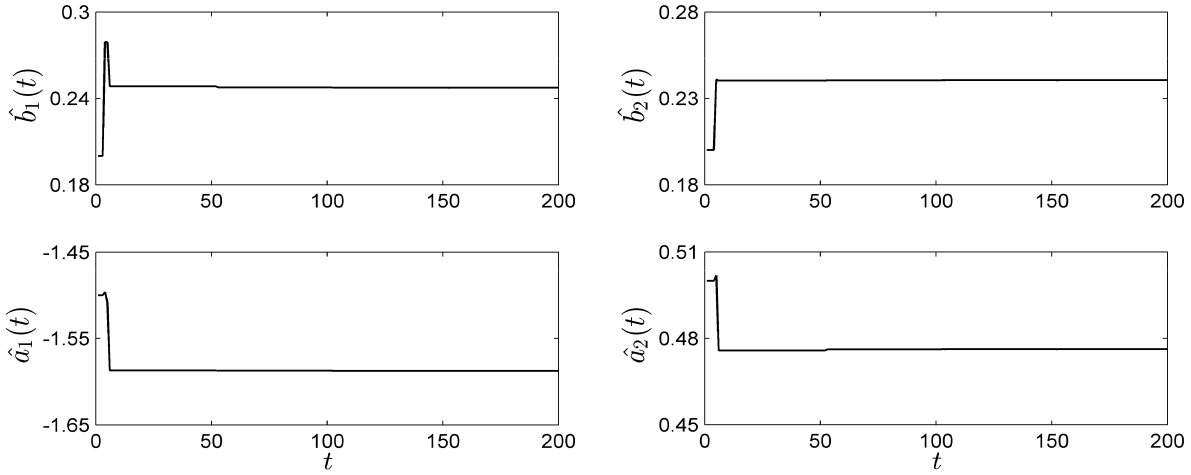

FIGURE 3. The parameter estimates $\hat{\theta}(t)$.

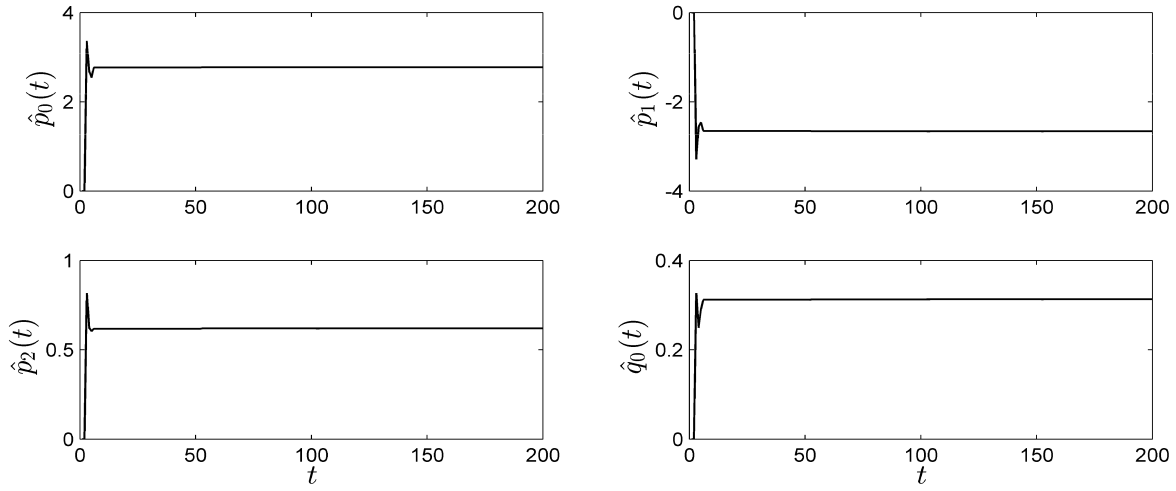

FIGURE 4. The values of $\hat{p}_0(t)$, $\hat{p}_1(t)$, $\hat{p}_2(t)$ and $\hat{q}_0(t)$.

The unmodeled dynamics consists of two parts $\zeta(t) = \zeta_1(t) + \zeta_2(t)$, where $\zeta_1(t) = \frac{0.1u(t)+0.05y(t)}{\sqrt{1+u(t)^2+y(t)^2}}$ and $\zeta_2(t) \sim N(0, 0.05^2)$. It is clear that $\zeta(t)$ is bounded.

The proposed RIASMC method is applied to control this nonlinear system. The orders are $n_a = n_b = 2$. The weighting polynomials are $\hat{P}(t, z^{-1}) = \hat{p}_0(t) + \hat{p}_1(t)z^{-1} + \hat{p}_2(t)z^{-2}$, $\hat{Q}(t, z^{-1}) = \hat{q}_0(t)(1 - z^{-1})$ and $\hat{R}(t) = \hat{p}_0(t) + \hat{p}_1(t) + \hat{p}_2(t)$. The initializations are $\varepsilon = 1.5$, $\bar{\chi} = 1.05$, $r(0) = 1$, $\hat{\sigma}(0) = 0$, $\hat{\theta}(0) = \left[0.2,\ 0.2\,,\ -1.5\,,\ 0.5\right]^T$ and $\Gamma(z^{-1}) = \left(1 - 0.4z^{-1}\right)^2$. The reference is designed to be

$$y^*(t) = \begin{cases} 1, & 0 < t \le 50, \quad 100 < t \le 150 \\ -1, & \text{otherwise} \end{cases}$$

Fig. 2 shows the output response $y(t)$ versus the reference $y^*(t)$, and the control input $u(t)$. Fig. 3 shows the estimation results of $\hat{\theta}(t)$. Fig. 4 shows the updates of $\hat{p}_0(t)$, $\hat{p}_1(t)$, $\hat{p}_2(t)$ and $\hat{q}_0(t)$. Fig. 5 shows the estimates of the upper bound $\hat{\sigma}(t)$, the estimates of $\hat{\zeta}(t)$, and the actual model error $e(t)$.

Overall, it can be seen that the closed-loop system is stable, the system output tracks the reference rapidly, all the estimates approach a bounded interval, and the noise rejection ability is reliable.

The results have confirmed Theorem 1 since all the signals are uniformly bounded and the system output $y(t)$ approaches a small region of the reference $y^*(t)$ under stochastic noises. Although $\hat{\theta}(0) = \left[0.2,\ 0.2\,,\ -1.5\,,\ 0.5\right]^T$ is not equal to the system parameter $\theta = \left[0.25,\ 0.3\,,\ -2\,,\ 0.8\right]^T$, the recursive estimator is able to cope with the uncertainties by updating the controller parameters online. However, it is a consensus that adaptations need enough excitations. Thus it is also found that there exist undesirable overshoot and oscillation at the beginning period, which is inevitable and acceptable.

The relation $\lim_{t\to\infty} \sup \left\{|e(t)| - \hat{\sigma}(t-1)\right\} \le 0$ is reflected in Fig. 5, which demonstrates that although the upper bound of the unmodeled dynamics is unknown, the recursive estimator with a deadzone factor can still be constructed. When the

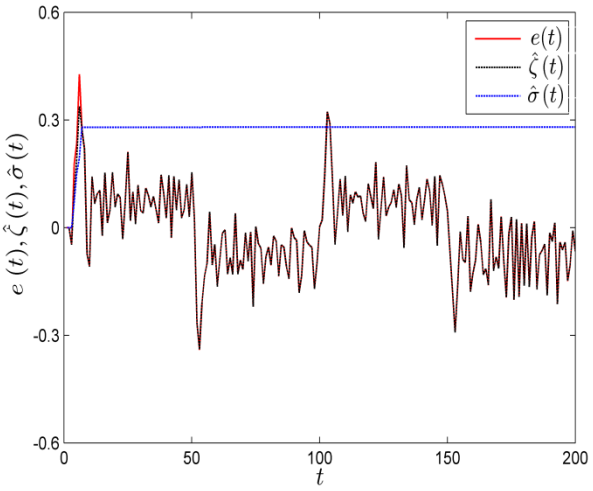

FIGURE 5. The estimates $\hat{\sigma}(t)$ and $\hat{\zeta}(t)$ versus the model error $e(t)$.

operation condition is changed, the relation $|e(t)| > \hat{\sigma}(t-1)$ is satisfied and therefore the recursive estimator works; while at the steady state, the model error $e(t)$ is gradually governed by the upper bound $\hat{\sigma}(t)$ and then the recursive estimator stops working.

Moreover, the property $\lim_{t\to\infty} |\hat{\zeta}(t)| = \lim_{t\to\infty} |e(t)|$ has also been verified in Fig. 5, which indicates that the effects of the unmodeled dynamics $\zeta(t)$ can be compensated by $\hat{\zeta}(t)$. Even though the robust design may reduce the adaptive performance, this additional compensation control can improve the output tracking performance in time.

VI. APPLICATION TO THE CONTROL PROBLEM OF A SMA ACTUATOR SYSTEM

A. EXPERIMENTAL SETUP

The experimental platform diagram of the SMA actuator is displayed in Fig. 6, and the picture of the experimental setup is given in Fig. 7. The structure of this SMA actuated system is similar to the ones in [34] and [37] but without a cooling device. The wire of SMA is the Flexinol actuator wire which is produced by Dynalloy, Inc. For this type of wire, the diameter is $0.00025m$, the length is $0.34m$, the deformations are up to 4%, and the Austenite finish temperature is 90ř. In this experiment, the system output is the displacement (unit: m) and the input signal is the current (unit: A), which is constrained to the range $0 \sim 0.4$. The control current applied to the SMA actuator is obtained from a V/I converter. The SMA wire then generates significant strains in response to the temperature changes which is caused by the current heating effect. The displacement of the SMA wire is measured by a high precision potentiometer. The Beckhoff ethercat terminals are used for the transformation and the conversion of data, and the sample frequency is 200Hz. In order to deform the SMA and achieve actuations, various loads are added to this system. The nominal models are established under the condition that the load is fixed as $500g$.

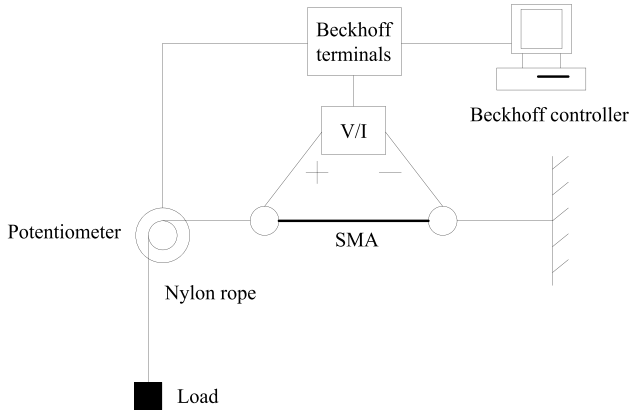

FIGURE 6. The experimental platform diagram of the SMA actuator.

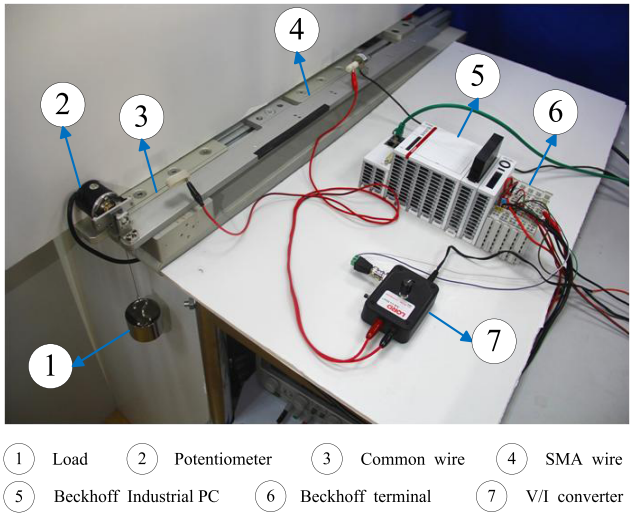

FIGURE 7. The experimental setup of the SMA actuated system.

B. A MECHANISM MODEL BASED CONTROLLER DESIGN

In the literature, the nonlinear modeling strategy of a SMA actuator has long been an open problem. In [34]–[36], [40], and [41], nonlinear dynamics of SMA actuators have been successfully described by some mechanism models.

In the comparison study, the utilized model is based on the mechanism model in [28] which has been recently established by our research team. This model is consisted of the following parts: a thermal model, a phase transformation model, and a description of the mechanical properties and dynamics of the system. Due to lack of space, the analysis procedure is omitted here and please refer to [28, Sec. 2] for details.

The mechanism model is described as follow

$$\dot{x} = f(x) + g(x)\widehat{u} \tag{54}$$

$$y = x_2 \tag{55}$$

where $x = [x_1, x_2, x_3]^T$; $x_1 = T - T_{amb}$; x_2 is the displacement of the SMA wire; x_3 is the instantaneous velocity, *i.e.*$x_3 = \dot{x}_2$; the functions $f(x)$ and $g(x)$ contain uncertain coefficients; y is the output; $\widehat{u}$ is the auxiliary control signal,

which is defined as the square of the current signal $\widehat{u} = i^2$ and is constrained to the range $0 \sim 0.16$.

The feedback linearization control (FLC) approach has been designed based on the mechanism model (54)-(55). Firstly, by the definition of the extended state variable $z = [x_2, x_3, \dot{x}_3]^T$, the nonlinear system is transformed to the equivalent linear system $\dot{z} = A_c z + B_c v$. Then based on this linear system, the control law for the extended control signal v can be designed. Finally, by the use of the inverse transformation, the auxiliary control signal $\widehat{u}$ and the actual control signal i can be easily calculated. This mechanism model based FLC scheme will be used for the following experiments as a comparison.

C. A GRAY-BOX MODEL BASED CONTROLLER DESIGN

As an alternative, the proposed RIASMC method requires no mechanism model. Instead, a gray-box model (2) is used to simplify the controller design procedure. Interestingly, for this scheme, only the input current and the output displacement are measured, and no other information is needed.

For the model (2), the orders are $n_a = n_b = 2$. The weighting polynomials are $\hat{P}(t, z^{-1}) = \hat{p}_0(t) + \hat{p}_1(t)z^{-1} + \hat{p}_2(t)z^{-2}$, $\hat{Q}(t, z^{-1}) = \hat{q}_0(t)(1 - z^{-1})$ and $\hat{R}(t) = \hat{p}_0(t) + \hat{p}_1(t) + \hat{p}_2(t)$. The initializations are as follows: $\varepsilon = 0.3$, $\bar{\chi} = 1.01$, $r(0) = 1$, $\hat{\sigma}(0) = 0$ and $\Gamma(z^{-1}) = 1 - 0.97z^{-1}$.

An important issue is to determine $\hat{\theta}(0)$ prior to the online implementation. The excitations come from some input-output data around different operating points. The identified model is defined as $y(t+1) \triangleq \varphi^T(t+1)\hat{\theta}(t)$. The recursive identification algorithms $\hat{\theta}(t) = \hat{\theta}(t-1) + \frac{P(t-1)\varphi(t)\left[y(t)-\varphi^T(t)\hat{\theta}(t-1)\right]}{1+\varphi^T(t)P(t-1)\varphi(t)}$ and $P(t) = P(t-1) - \frac{P(t-1)\varphi(t)\varphi^T(t)P(t-1)}{1+\varphi^T(t)P(t-1)\varphi(t)}$ are used. Then a good initialization is obtained and the convergent result is $\hat{\theta}(0) = \left[-0.00934, 0.00921, -0.499, -0.499\right]^T$. Note that this procedure is offline realized in the Matlab software.

Based on the above initializations, the RIASMC method now can be applied to control this system. The parameter adjusting is (12)-(18), and the control law adaptation is (20). Some remarks are as follows: (i) It is clear that the dimension of $\varphi(t)$ and $\hat{\theta}(t)$ is 4. The recursive identification algorithm is based on a stochastic gradient algorithm which requires no inverse matrix calculation. Therefore the recursive estimator requires low computational burden and is usable for the online control; (ii) The weighing polynomials updating is employed for the purpose of fast output response when the operation condition changes, while the coefficients of the weighing polynomials is fixed as $\hat{p}_0(t) = 1.035$, $\hat{p}_1(t) = -0.5125$, $\hat{p}_2(t) = -0.5144$and $\hat{q}_0(t) = 0.01$for robustness considerations under load variations and stochastic disturbances.

D. SET-POINT TRACKING

Two groups of set-point tracking experiments are conducted based on different loads. In Fig. 8, the load is fixed as $500g$; while for Fig. 9, the load is fixed as 700g.

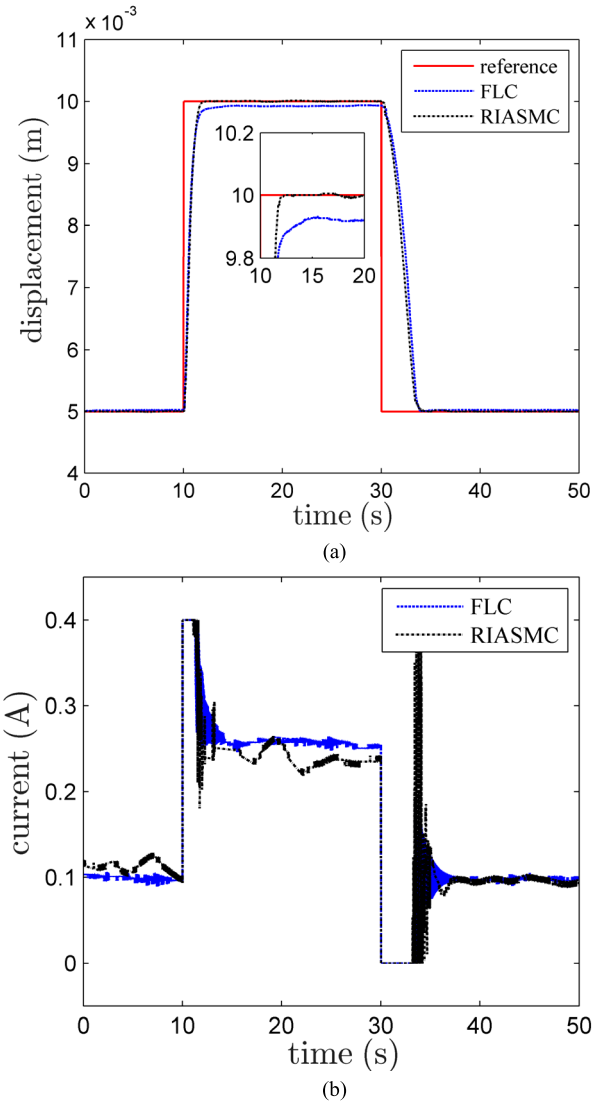

FIGURE 8. The set-point tracking results by these two control schemes (the load is 500g). (a) The system output. (b) The control input.

From the results, it is seen that the performance of the FLC method is poorer, especially for the tracking errors. It indicates that there exists unmodeled dynamics in the nonlinear model (54)-(55), but the FLC method cannot compensate the negative effects. In general, it is a consensus that mechanism models can hardly describe the nonlinear dynamics of complex industrial processes.

On the other hand, the RIASMC method can ensure desirable performance in the sense that the closed-loop system is stable, the tracking error is very small, the response is fast enough, the overshoot and oscillation are limited, and the control input is reasonable. These results have verified the effectiveness of the proposed control scheme.

The performance of the RIASMC method is better than the FLC method except for the continuous fluctuations of the input signals. The oscillations are mainly caused by the robust design concept, which have made the RIASMC scheme

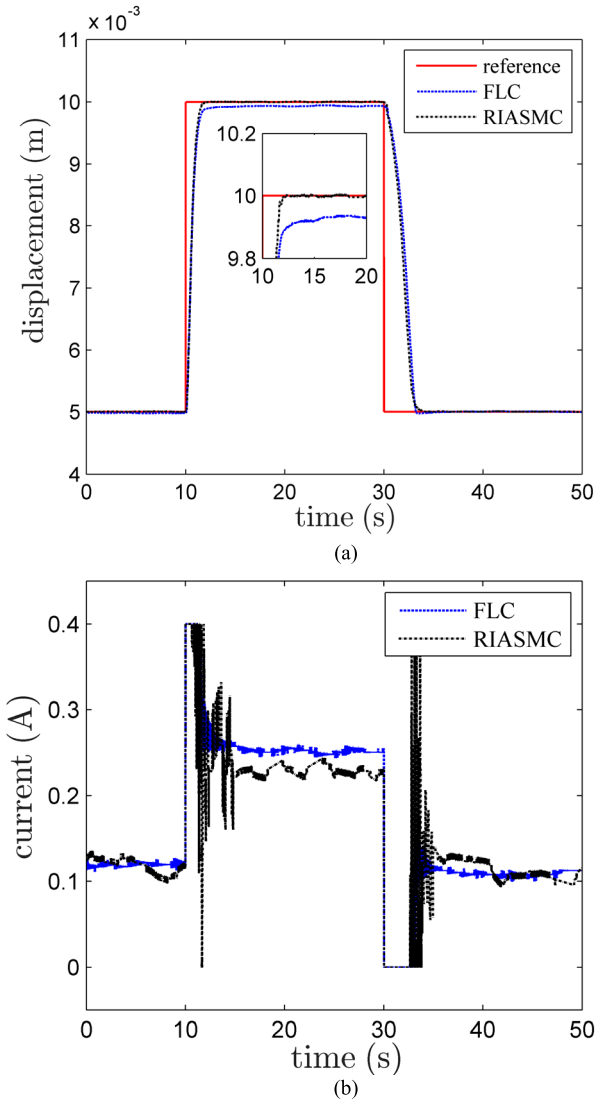

FIGURE 9. The set-point tracking results by these two control schemes (the load is 700g). (a) The system output. (b) The control input.

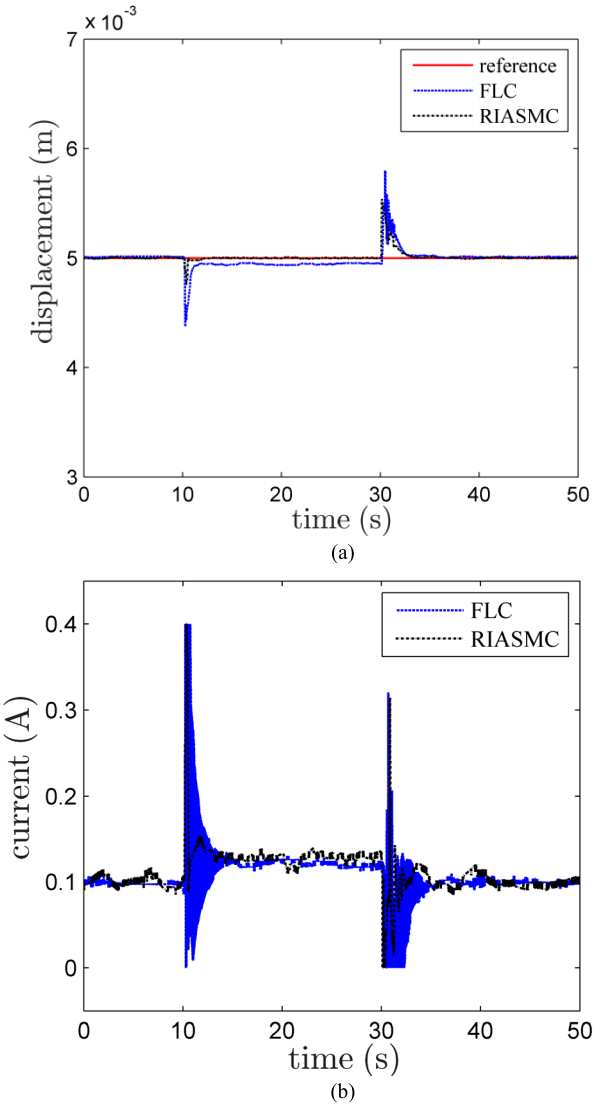

FIGURE 10. The regulation results under the load variations by these two control schemes (an additional 200g load is added to this system at 10th second and removed at 30th second). (a) The system output. (b) The control input.

become a bit more conservative. For many specific applications in the field of rehabilitation robots [44], which demand reliable robustness property for safety considerations, such kind of compromise is reasonable and necessary.

It is found that the same set-point corresponds to different control input signals. This is caused by the inherent hysteresis phenomena of SMAs. Moreover, it is also found that the control input signals vary a lot. This is because that the actuations are affected by the ambient temperatures, which are uncertain and unmeasurable.

E. LOAD VARIATIONS

Three groups of load variations experiments are conducted. in which there exist different levels of parametric uncertainties. In Figs. 10-11, additional loads are added to the SMA actuator system at 10th second, and removed at 30th second. In Fig. 12, instantaneous forces are imposed on this system. The regulation results are tested at the set-point $y^*(t) = 0.005m$.

Although the FLC method ensures the closed-loop system stability, this controller seems ineffective for the load variations experiments. In Figs. 10-11, when the load increases to $700g$ or $1000g$, this system corresponds to a different mechanism model. It is obvious that, during the 10th second to 30th second, there exist unsatisfactory regulation errors. This is because that the FLC method is non-adaptive and thus can hardly cope with the parametric uncertainties caused by load variations. While for Fig. 12, when unknown instantaneous vertical forces are added, the mathematical description of this system remains unchanged. But there appear pulse signals at 10th second and 30th second, which induce sudden tracking errors into this system. From the results, it is seen that the overshoot is severe and the regulation time is long, which indicates that the robustness property of the FLC method is poor.

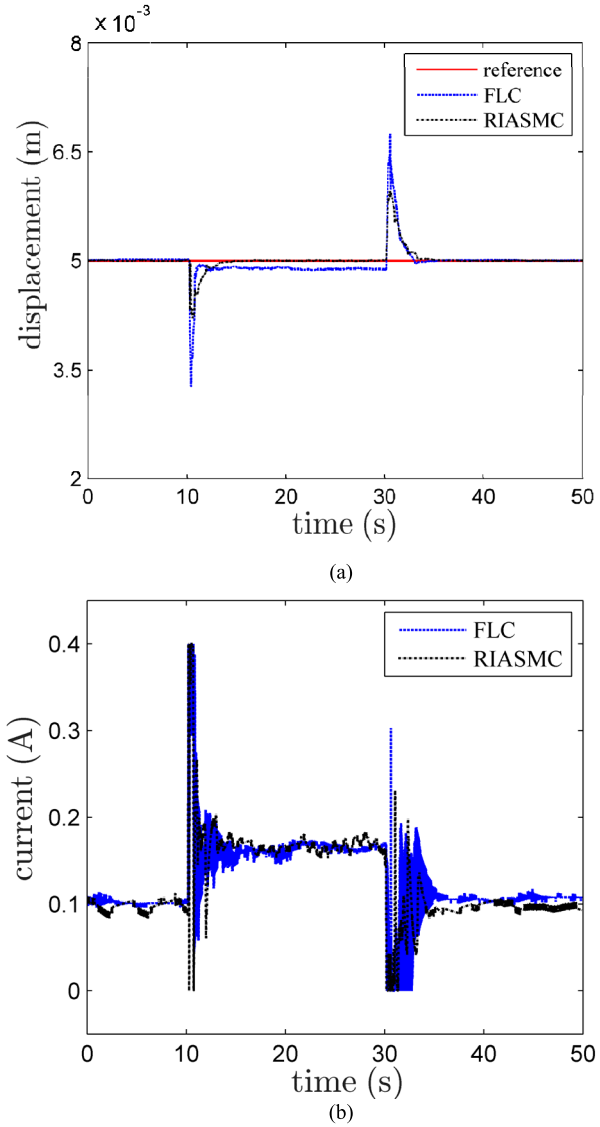

FIGURE 11. The regulation results under the load variations by these two control schemes (an additional 500g load is added to this system at 10th second and removed at 30th second). (a) The system output. (b) The control input.

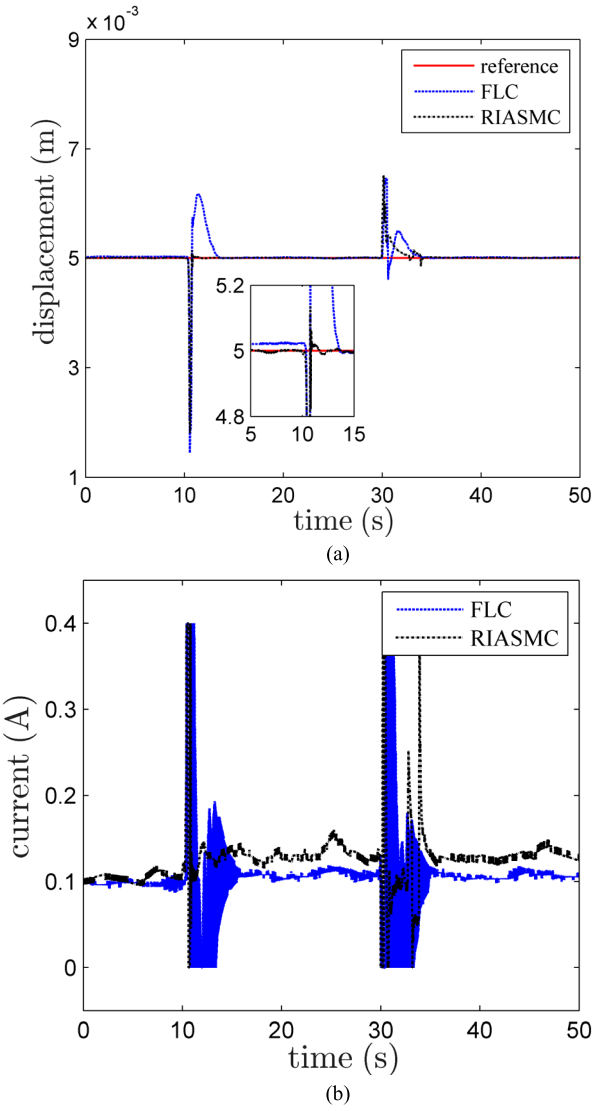

FIGURE 12. The regulation results under instantaneous forces by these two control schemes (an downward vertical force is instantaneously added to this system at 10th second, and later an upward vertical force is instantaneously added to this system at 30th second). (a) The system output. (b) The control input.

On the other hand, the RIACMC method is effective under load variations. It is found that the closed-loop system is stable, the regulation time is acceptable, and the overshoot is small. The results indicate that the RIASMC method has made a more reasonable compromise between the adaptive performance and the system robustness. Thanks to the dead-zone weighted factor (14), this controller is more reliable. Meanwhile, the additional compensation control increases the response speed.

It is a fact that load variations can cause uncertainties in most robotic manipulators [45]. However, many mechanism models based strategies have fixed controller parameters, which cause inevitable performance deteriorations. Alternatively, adaptive controllers address the uncertainties effectively and seem to be more favorable.

F. STOCHASTIC DISTURBANCES

In order to test the disturbance rejection ability, an unknown lateral force is suddenly imposed to the load. This can cause a continuous non-Gaussian stochastic noise to the system output over a period of time.

Figs. 13-14 show the noise rejection results. The root mean square errors (RMSE) $\left\{\frac{1}{N}\sum_{t=1}^{N}\left(y\left(t\right)-y^{*}\left(t\right)\right)^{2}\right\}^{1/2}$ and the mean absolute difference (MAD) $\frac{1}{N}\sum_{t=1}^{N}\left|y\left(t\right)-y^{*}\left(t\right)\right|$ have also been given in Figs. 13-14.

It can be found that the RIASMC method is still stable under a continuous non-Gaussian noise, and the disturbance rejection ability is reliable. It also indicates that the robust estimator and the compensation control not only improve the

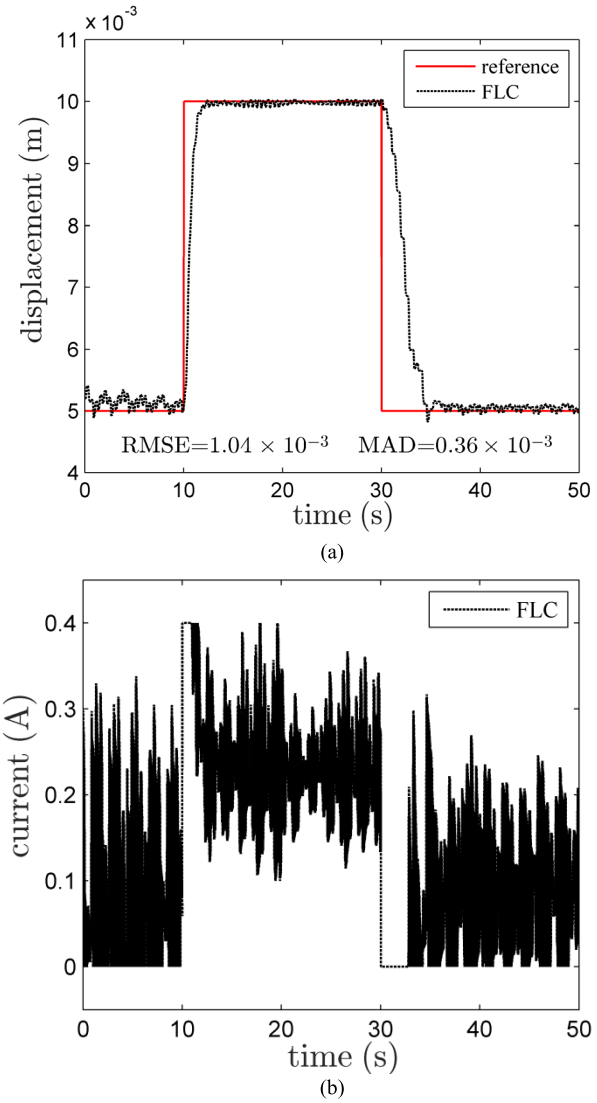

FIGURE 13. The disturbance rejection results under the continuous stochastic noise by the FLC control scheme. (a) The system output. (b) The control input.

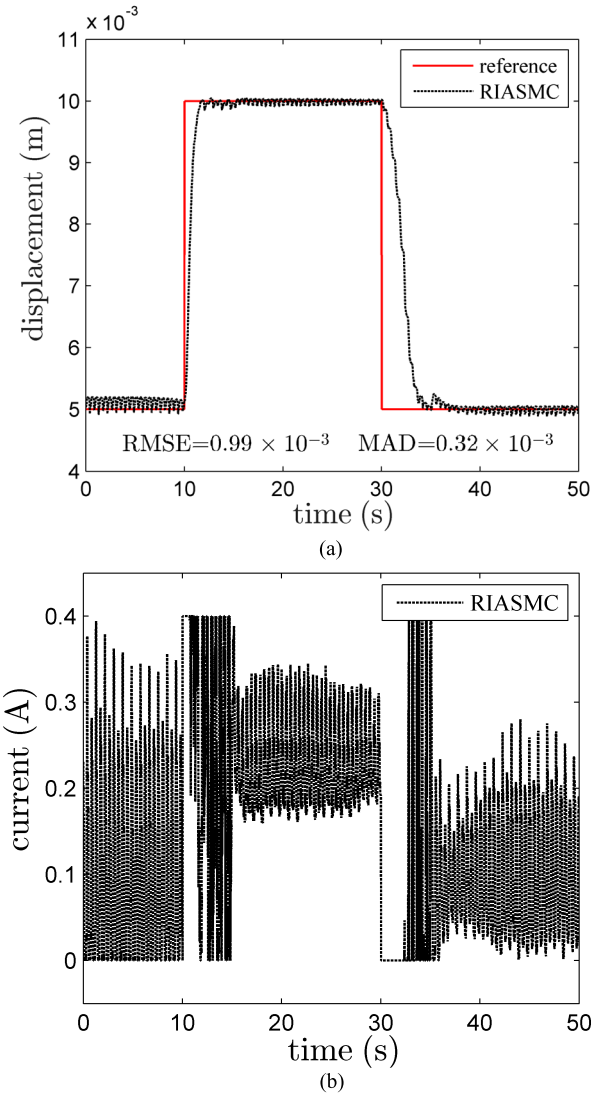

FIGURE 14. The disturbance rejection results under the continuous stochastic noise by the RIASMC control scheme. (a) The system output. (b) The control input.

performance in a deterministic case but also benefit the noise rejection ability in a stochastic case.

On the other hand, the disturbance rejection performance of the FLC method is limited. Plenty of experimental results show that the regulations are often very sluggish and the control input signals fluctuate severely.

G. SUMMARY

The FLC method is quite sensitive to unmodeled dynamics, let alone load variations and stochastic disturbances. Although the closed-loop stability can be guaranteed under uncertainties, the control performance is unsatisfactory.

Generally speaking, the RIASMC method has much wider applicability especially for its improved performance, smoother adaptation and reliable robustness.

In addition, another salient feature of this gray-box model based control strategy is that the design procedure is much more convenient than some existing mechanism model based control schemes.

Note that the RIASMC method is also sensitive to the initial condition $\hat{\theta}(0)$, which is the main limitation of this controller. But this issue does not affect the applicability. In general, for an unfamiliar plant, the system identification is always possible to be conducted based on some historical input-output data, prior to the controller implementation. Consequently, a satisfactory initialization $\hat{\theta}(0)$ is available in practice and can be applied to this adaptive controller.

VII. CONCLUSION

This paper introduces a novel robust indirect adaptive sliding mode control strategy for nonlinear systems with uncertainties. The controller is consisted of four parts: the system parameters estimation, the unmodeled dynamics estimation, the weighting polynomials updating and the control law calculation. For the theoretical aspects, the main merits are

summarized as follows: (i) the controller is applicable to non-minimum phase and open- loop unstable systems; (ii) the estimation of the unmodeled dynamics is introduced as a feedback compensation control to improve the response; (iii) the strict stability condition is eliminated and a desirable closed-loop performance is ensured during a wide operation region. For the practical application aspects, the proposed controller is further applied to the control problem of a SMA actuator. Without mechanism models, this controller is designed based on a gray-box model, in which only the input current and the output displacement are required. This controller is explicit and reliable, and has been implemented through the Beckhoff controller. The comparison results have demonstrated that the proposed robust adaptive controller has wider applicability than some existing methods, especially for its improved performance, smoother adaptation and reliable robustness. In the future, it is desired that the obtained results could find further applicability in SMA-actuated rehabilitation robots.

REFERENCES

[1] W. Sun, Y. Zhang, Y. Huang, H. Gao, and O. Kaynak, "Transient-performance-guaranteed robust adaptive control and its application to precision motion control systems," *IEEE Trans. Ind. Electron*, vol. 63, no. 10, pp. 6510–6518, Oct. 2016.

[2] G. C. Goodwin and K. S. Sin, *Adaptive Filtering Prediction and Control*. Englewood Cliffs, NJ, USA: Prentice-Hall, 1984.

[3] G. Goodwin, P. J. Ramadge, and P. E. Caines, "Discrete-time multivariable adaptive control," *IEEE Trans. Autom. Control*, vol. 25, no. 3, pp. 449–456, Jun. 1980.

[4] G. C. Goodwin, P. J. Ramadge, and P. Caines, "Discrete time stochastic adaptive control," *SIAM J. Control Optim.*, vol. 20, no. 6, pp. 829–853, 1982.

[5] G. C. Goodwin and K. S. Sin, "Adaptive control of non-minimum phase systems," *Int. J. Adapt. Control Signal Process.*, vol. 9, no. 2, pp. 478–483, 1981.

[6] T. Y. Chai, "A self-tuning decoupling controller for a class of multivariable systems and global convergence analysis," *IEEE Trans. Autom. Control*, vol. 33, no. 8, pp. 767–771, Aug. 1988.

[7] L. Guo and H.-F. Chen, "The AAstrom-Wittenmark self-tuning regulator revisited and ELS-based adaptive trackers," *IEEE Trans. Autom. Control*, vol. 36, no. 7, pp. 802–812, Jul. 1991.

[8] F.-C. Chen and H. K. Khalil, "Adaptive control of a class of nonlinear discrete-time systems using neural networks," *IEEE Trans. Autom. Control*, vol. 40, no. 5, pp. 791–801, May 1995.

[9] K. S. Narendra and S. Mukhopadhyay, "Adaptive control of nonlinear multivariable systems using neural networks," *Neural Netw.*, vol. 7, no. 5, pp. 737–752, 1994.

[10] R. Qi, G. Tao, and B. Jiang, "Adaptive control of MIMO time-varying systems with indicator function based parametrization," *Automatica*, vol. 50, no. 5, pp. 1380–1396, 2014.

[11] R. Qi, G. Tao, B. Jiang, and C. Tan, "Adaptive control schemes for discrete-time T–S fuzzy systems with unknown parameters and actuator failures," *IEEE Trans. Fuzzy Syst.*, vol. 20, no. 3, pp. 471–486, Jun. 2011.

[12] K. S. Narendra and J. Balakrishnan, "Adaptive control using multiple models," *IEEE Trans. Autom. Control*, vol. 42, no. 2, pp. 171–187, Feb. 1997.

[13] Z. Han and K. S. Narendra, "New concepts in adaptive control using multiple models," *IEEE Trans. Autom. Control*, vol. 57, no. 1, pp. 78–89, Jan. 2012.

[14] R. Rout and B. Subudhi, "NARMAX self-tuning controller for line-of-sight-based waypoint tracking for an autonomous underwater vehicle," *IEEE Trans. Control Syst. Technol.*, vol. 25, no. 4, pp. 1529–1536, Jul. 2017.

[15] W.-X. Zhao and H.-F. Chen, "Adaptive tracking and recursive identification for Hammerstein systems," *Automatica*, vol. 45, no. 12, pp. 2773–2783, 2009.

[16] W. R. Cluett, J. M. Martin-Sanchez, S. L. Shah, and D. G. Fisher, "Stable discrete-time adaptive control in the presence of unmodeled dynamics," *IEEE Trans. Autom. Control*, vol. 33, no. 4, pp. 410–414, Apr. 1988.

[17] X. Y. Gu and W. Wang, "On the stability of a self-tuning controller in the presence of bounded disturbances," *IEEE Trans. Autom. Control*, vol. 34, no. 2, pp. 211–214, Feb. 1989.

[18] J. Yao, W. Deng, and W. Sun, "Precision motion control for electro-hydraulic servo systems with noise alleviation: A desired compensation adaptive approach," *IEEE/ASME Trans. Mechatronics*, vol. 22, no. 4, pp. 1859–1868, Aug. 2017.

[19] L. Chen and K. S. Narendra, "Nonlinear adaptive control using neural networks and multiple models," *Automatica*, vol. 37, no. 8, pp. 1245–1255, Aug. 2001.

[20] A. Bartoszewicz and R. J. Patton, "Sliding mode control," *Int. J. Adapt. Control Signal Process.*, vol. 21, nos. 8–9, pp. 635–637, 2007.

[21] K. Furuta, "VSS type self-tuning control," *IEEE Trans. Ind. Electron.*, vol. 40, no. 1, pp. 37–44, Feb. 1993.

[22] P.-M. Lee and J.-H. Oh, "Improvements on VSS-type self-tuning control for a tracking controller," *IEEE Trans. Ind. Electron.*, vol. 45, no. 2, pp. 319–325, Apr. 1998.

[23] X. Chen, T. Fukuda, and K. D. Young, "Adaptive quasi-sliding-mode tracking control for discrete uncertain input-output systems," *IEEE Trans. Ind. Electron.*, vol. 48, no. 1, pp. 216–224, Feb. 2001.

[24] X. Chen, "Adaptive sliding mode control for discrete-time multi-input multi-output systems," *Automatica*, vol. 42, no. 3, pp. 427–435, Mar. 2006.

[25] X. Chen, T. Hisayama, and C.-Y. Su, "Pseudo-inverse-based adaptive control for uncertain discrete time systems preceded by hysteresis," *Automatica*, vol. 45, no. 2, pp. 469–476, 2009.

[26] X. Chen and T. Hisayama, "Adaptive sliding-mode position control for piezo-actuated stage," *IEEE Trans. Ind. Electron.*, vol. 55, no. 11, pp. 3927–3934, Nov. 2008.

[27] T. Y. Chai, "An indirect stochastic adaptive scheme with on-line choice of weighting polynomials," *IEEE Trans. Autom. Control*, vol. 35, no. 1, pp. 82–85, Jan. 1990.

[28] X. G. Li, D. H. Zhang, X. G. Zhao, and J. D. Han, "Modeling and control of shape memory alloy actuator using feedback linearization," in *Proc. 36th Chin. Control Conf. (CCC)*, Dalian, China, Jul. 2017, pp. 1222–1227.

[29] M. H. Elahinia, H. Ashrafiuon, M. Ahmadian, and H. G. Tan, "A temperature-based controller for a shape memory alloy actuator," *J. Vib. Acoust.*, vol. 127, no. 3, pp. 285–291, 2005.

[30] E. Henderson, D. H. Nash, and W. M. Dempster, "On the experimental testing of fine Nitinol wires for medical devices," *J. Mech. Behav. Biomed. Mater.*, vol. 4, no. 3, pp. 261–268, 2011.

[31] R. Mehrabi and M. Kadkhodaei, "3D phenomenological constitutive modeling of shape memory alloys based on microplane theory," *Smart Mater. Struct.*, vol. 22, no. 2, pp. 17–25, 2013.

[32] S. Dieter, "Shape memory actuator for automotive applications," *Mater. Des.*, vol. 11, no. 6, pp. 302–307, 1990.

[33] M. M. Kheirikhah, S. Rabiee, and M. E. Edalat, *A Review of Shape Memory Alloy Actuators in Robotics*. Berlin, Germany: Springer, 2011, pp. 206–217.

[34] R. Romano and E. A. Tannuri, "Modeling, control and experimental validation of a novel actuator based on shape memory alloys," *Mechatronics*, vol. 19, no. 7, pp. 1169–1177, 2009.

[35] H. Ashrafiuon and V. R. Jala, "Sliding mode control of mechanical systems actuated by shape memory alloy," *ASME J. Dyn. Syst. Meas. Control*, vol. 131, no. 1, pp. 101–116, 2009.

[36] A. Pai, M. Riepold, and A. Trächtler, "Model-based precision position and force control of SMA actuators with a clamping application," *Mechatronics*, vol. 50, pp. 303–320, Apr. 2018.

[37] N. T. Tai and K. Y. Ahn, "A RBF neural network sliding mode controller for SMA actuator," *Int. J. Control Autom. Syst.*, vol. 8, no. 6, pp. 1296–1305, 2010.

[38] J. H. Wiest and G. D. Buckner, "Indirect intelligent sliding mode control of antagonistic shape memory alloy actuators using hysteretic recurrent neural networks," *IEEE Trans. Control Syst. Technol.*, vol. 22, no. 3, pp. 921–929, May 2014.

[39] N. Nikdel, P. Nikdel, M. A. Badamchizadeh, and I. Hassanzadeh, "Using neural network model predictive control for controlling shape memory alloy-based manipulator," *IEEE Trans. Ind. Electron.*, vol. 61, no. 3, pp. 1394–1401, Mar. 2014.

[40] M. R. Zakerzadeh and H. Sayyaadi, "Precise position control of shape memory alloy actuator using inverse hysteresis model and model reference adaptive control system," *Mechatronics*, vol. 23, no. 8, pp. 1150–1162, 2013.
[41] L. Riccardi, D. Naso, B. Turchiano, and H. Janocha, "Adaptive control of positioning systems with hysteresis based on magnetic shape memory alloys," *IEEE Trans. Control Syst. Technol.*, vol. 21, no. 6, pp. 2011–2023, Nov. 2013.
[42] Y. Pan, Z. Guo, X. Li, and H. Yu, "Output-feedback adaptive neural control of a compliant differential SMA actuator," *IEEE Trans. Control Syst. Technol.*, vol. 25, no. 6, pp. 2202–2210, Nov. 2017.
[43] A. Patete, K. Furuta, and M. Tomizuka, "Self-tuning control based on generalized minimum variance criterion for auto-regressive models," *Automatica*, vol. 44, no. 8, pp. 1970–1975, 2008.
[44] Z. G. Hou, X. G. Zhao, L. Cheng, Q. N. Wang, and W. Q. Wang, "Recent advances in rehabilitation robots and intelligent assistance systems," *Acta Automatica Sinica*, vol. 42, no. 12, pp. 1765–1779, 2016.
[45] D. Zhang, X. Zhao, and J. Han, "Active model-based control for pneumatic artificial muscle," *IEEE Trans. Ind. Electron.*, vol. 64, no. 2, pp. 1686–1695, Feb. 2016.

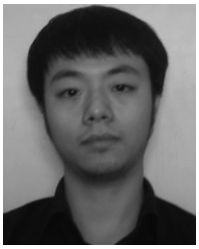

BI ZHANG received the Ph.D. degree in control theories and control applications from Northeastern University, Shenyang, China. He is currently an Assistant Professor with the State Key Laboratory of Robotics, Shenyang Institute of Automation, Chinese Academy of Sciences. His recent research interests are advanced control theories and their applications in rehabilitation robots.

XIN-GANG ZHAO was born in Tai'an, Shandong, China, in 1978. He received the B.E. and M.E. degrees in mechanics from Jilin University, Changchun, China, in 2000 and 2004, respectively, and the Ph.D. degree in pattern recognition and intelligent systems from the Chinese Academy of Sciences, Shenyang, China, in 2008. From 2015 to 2016, he was a Visiting Scientist with the Rehabilitation Institute of Chicago, Chicago, IL, USA. He is currently a Professor with the State Key Laboratory of Robotics, Shenyang Institute of Automation, Chinese Academy of Sciences. His main research interests include medical robots, rehabilitation robots, robot control, and pattern recognition.

XIAO-GUANG LI is currently pursuing the Ph.D. degree with the State Key Laboratory of Robotics, Shenyang Institute of Automation, Chinese Academy of Sciences. She is also a Lecturer with the Shenyang University of Technology, China. Her recent research interests are modeling and control of smart actuator systems.

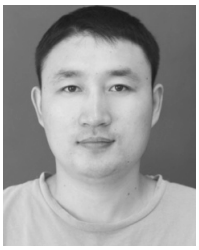

DAO-HUI ZHANG is currently an Assistant Professor with the State Key Laboratory of Robotics, Shenyang Institute of Automation, Chinese Academy of Sciences. His main research interests include nonlinear estimation and control, robotics, and pattern recognition.